Materials Research, Vol. 9, No. 1, 65-71, 2006

Microstructural Characterization and Interactions in Ti- and TiH_2-Hydroxyapatite Vacuum Sintered Composites

Teresa Maria Marcelo[a], Vanessa Livramento[a], Marize Varella de Oliveira[b], Maria Helena Carvalho[a]*

[a]*Instituto Nacional de Engenharia, Tecnologia e Inovação, Azinhaga dos Lameiros, 1649-038 Lisboa, Portugal*
[b]*Instituto Nacional de Tecnologia, Av. Venezuela, 82/602, 20081-312 Rio de Janeiro, Brazil*

Received: December 2, 2004; Revised: October 11, 2005

Titanium/hydroxyapatite (HAP) composites are candidate materials for biomedical applications as implants and hard tissue substitutes since they combine the good mechanical properties and biocompatibility of Ti with the excellent HAP bioactivity and osteointegration. In powder metallurgy processing of these composites, HAP decomposition promoted by Ti during powder sintering is found. In a previous work Ti-50v%HAP greens of 60% theoretical density (d_T) were vacuum sintered at 1150 °C and formation of CaO and $Ca_4O(PO_4)_2$ (TTCP) resulting from the HAP decomposition, as well as Ti_4P_3 at the Ti/HAP interfaces was obtained. In the present work those composites are compared with similar ones processed from TiH_2 as a substitute for Ti which were also vacuum sintered at 1150 °C from greens with 60 to 86%d_T. For the lower %d_T, the compounds formed were CaO, TTCP and Ti_4P_3 and for the higher %d_T ones, besides those same products, $CaTiO_3$, Ti_5P_3 and a phase containing Ti, Ca and P were detected.

Keywords: *titanium, TiH_2, hydroxyapatite, composites*

1. Introduction

The need for biocompatibility, bioactivity, osteointegration and adequate mechanical properties for dental and orthopedic implants has led to the development and effective clinical application of titanium alloys with or without hydroxyapatite coatings (HAP – $Ca_{10}(PO_4)_6(OH)_2$)[1,2]. In spite of the strong bond between the HAP coating and bone, one of the frequent problems of these coatings, usually produced by thermal spray deposition, is their weak adherence to the substrate[3]. In order to solve this problem Ti/HAP composite plasma-sprayed coatings, deposited on Ti substrates, have been studied[4]. Other Ti/HAP combinations have been considered recently, such as the functionally graded materials (FGM) and the homogeneous composites[5-10] fabricated by powder metallurgy (PM), with the purpose of optimizing both mechanical properties and biocompatibility. These composites have the ability to induce apatite nucleation and growth on its surface, when immersed in body fluid solution[9]. In addition, Ti/HAP FGM composites[5,6] can be designed to have a graded composition comparable to HAP coated Ti substrates but without the inconveniences associated to coating technologies and continuous interfaces.

As Ti is stable in vacuum or reducing atmospheres and HAP is stable only in oxidizing atmospheres[7], sintering of this type of composites is difficult and varied sintering conditions have been experimented[5,6,10]. Furthermore, results can not be extrapolated to processing from different raw materials, for which chemical and morphologic characteristics could lead to different sinterabilities and interactions. Detailed studies on characterization of the Ti/HAP interfaces in FGM or homogeneous PM composites were not found in the literature.

Aiming to produce later on Ti/HAP PM functionally graded composites it was decided to carry out previously an evaluation of the interactions between the constituents in homogeneous composites with 50 volume % of each constituent, using the Ti most favourable sintering conditions. Thus, composites were produced from TiH_2 with 50v%HAP sintered in vacuum at 1150 °C. The results are described in the present work and compared with those for equivalent composites processed from Ti powder[11].

2. Experimental

TiH_2 and HAP powders were produced by CTA (Centro Técnico Aeroespacial, Brazil) and CBPF (Centro Brasileiro de Pesquisas Físicas, Brazil), respectively. They were characterized through morphology evaluation (Scanning Electron Microscopy – SEM JEOL JSM-35CF, Japan), true density (He pycnometer Accupyc 1330, Micromeritics, USA), grain size distribution and mean particle size d_{50} (laser diffraction analyser 1064, CILAS, France) and X ray Diffraction (XRD) with CuK_α radiation (X ray Diffractometer D/MAX IIIC, Rigaku, Japan). Chemical analysis of the TiH_2 powder was carried out, the hydrogen content having been measured by infrared absorption (CHN 2000 analyser, LECO, USA). Dry powder mixing of TiH_2 with 50v%HAP was carried out in a Turbula mixer (T2C, Willy A. Bachofen AG, Switzerland). The mixture was compacted by Cold Isostatic Pressing (CIP National Forge Europe, Belgium) at 340 MPa in cylindrical moulds of 12 mm diameter and around 40 mm height; by uniaxial compaction (hydraulic press Carver, USA) in a 12 mm diameter die at pressures between 390 and 1180 MPa and by a combination of these two compaction procedures (uniaxial pressing of 10 mm ϕ x 6 mm height samples cut from the CIPed cylinders). The five different green geometrical densities (weight/volume) obtained varied from 60 to 86% of the mixture theoretical density (d_T), which is 3.21 $g.cm^{-3}$.

The green samples (duplicates of each compaction condition) were sintered in vacuum better than 10^{-3} Pa at 1150 °C for 2 hours (vacuum furnace Rubi 2201 W, LPA, France), with heating and cooling rates of 10 and 20 °C/min, respectively. After measuring the

*e-mail: teresa.marcelo@ineti.pt

sintered geometrical density as well as the true density on powdered samples, the microstructures and phases present were characterized through X ray (XR) maps and XR line profiles (Energy Dispersive Spectrometry EDS EDAX EDAM III, USA, associated to a SEM XL30 FEG, Philips, The Netherlands) obtained on mounted and polished samples, and through XRD of the powdered samples.

3. Results

Figure 1 shows the raw materials morphologies (loose powders); the observed HAP agglomerates could eventually have contributed to the d_{50} = 10 µm measured value; the corresponding d_{50} value for TiH_2 powder was 15 µm. The measured true densities of the HAP and TiH_2 powders were 2.8 and 3.6 $g.cm^{-3}$, respectively, lower than the tabled ones for their stoichiometric compositions.

XRD spectra of both powders are shown in Figure 2. The spectrum of the TiH_2 powder corresponds to the powder diffraction file[12] (PDF) of the tetragonal $TiH_{1.924}$, which is consistent with the amount of hydrogen measured (3.86 weight %). The other elements measured in the TiH_2 powder were (wt. (%)): 0.379 N, 0.177 O, 0.051 C, 0.061 Fe, 0.132 Cl, 0.05 Al, 0.364 Mg and 0.002 S.

The HAP powder was supplied as stoichiometric (chemical analysis not available) this being supported by XRD (Figure 2) since no other phases besides hydroxyapatite were detected[13] in the as-received powder nor in the HAP calcined at 1280 °C in air[13] and by FTIR analysis published elsewhere[11] (no HPO_4 detected).

The sintered composites exhibited a reasonably homogenous distribution of both constituents. As a result of the mixing process the HAP has formed larger agglomerates than those observed in the loose powder, which resulted in the two phase distribution shown in the typical microstructure illustrated in Figure 3. HAP zones with varied dimensions can be observed, dispersed in a matrix of Ti grains (former TiH_2). Darker zones disseminated in the Ti matrix can also be observed, which correspond mainly to the porosity that has not been eliminated during the sintering step.

As confirmed in preliminary tests, TiH_2 greens with about 82%d_T, sintered in the same conditions (1150 °C, 2 hours, vacuum), can reach full densification (Figure 4a). In the composites, in the areas where TiH_2 is predominant, sintering of these particles was affected by HAP fines that had originally separated the TiH_2 particles (interaction zones visible in Figure 4b); in the areas close to the large HAP agglomerates, the development of a porous phase in the interaction zone between Ti and HAP is observed (Figure 4c).

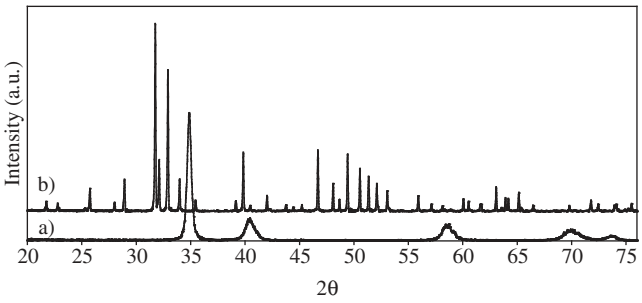

Figure 2. XRD spectra of the raw materials: a) TiH_2 as-received (PDF 25-0983 $TiH_{1.924}$); and b) HAP – as-received and as-calcined at 1280 °C (PDF 9-0432).

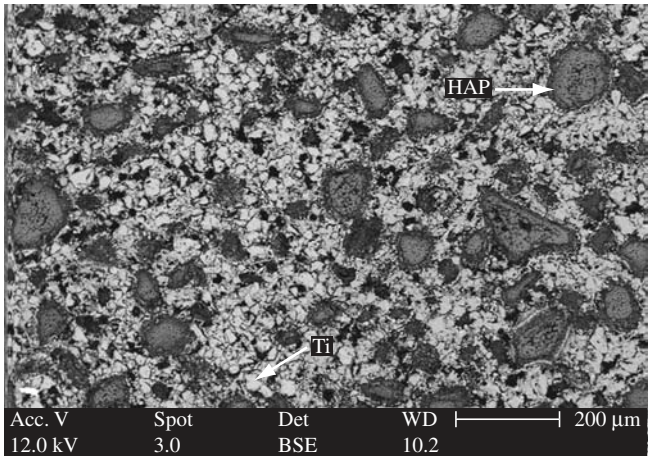

Figure 3. Typical microstructure (SEM) of the Ti/HAP composites sintered from TiH_2/50v%HAP (86%d_T).

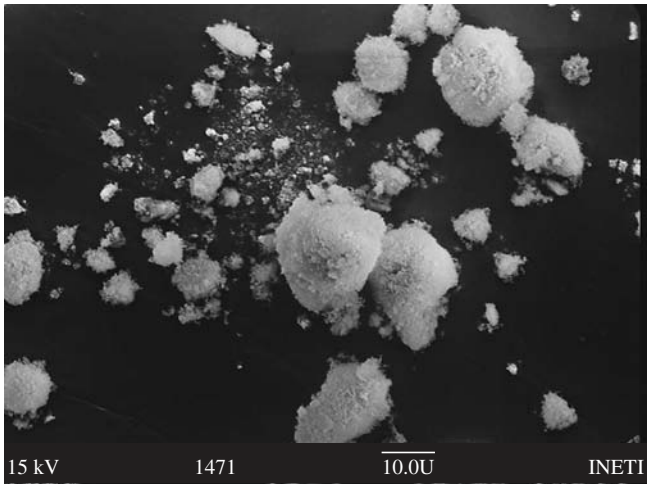

(a)

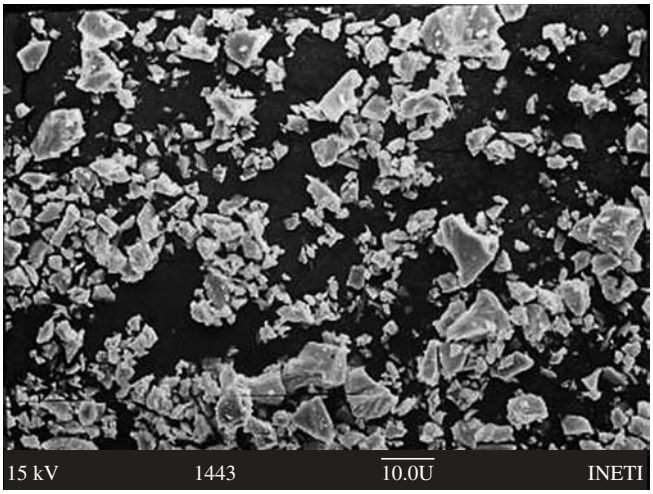

(b)

Figure 1. Morphology of the raw materials (SEM): a) HAP; and b) TiH_2.

By observing the microstructures at magnifications ≥ 2000x, as in Figure 4b) for example, the formation of new phases is evident. EDS analysis allowed the identification, in all composites, of a phase containing Ti and P at the Ti grain boundaries, with variable thickness and containing some porosity in the thicker layers. In the composites sintered from greens with 75%d_T or higher, it was also detected the presence of a phase with Ti and Ca in thin non porous layers, usually surrounding layers containing Ti and P and joining adjacent Ti grains, and another phase with Ti, Ca and P, which appears sporadically. These phases can be seen in Figures 5 and 6 through Ti, Ca and P XR maps and XR line profiles, respectively. The presence of phases with Ti and P (1) and Ti and Ca (2) is visible in Figures 5 and 6a) while the phase with Ti, Ca and P (3) can be identified in Figure 6b). As shown in the XRD spectrum presented in Figure 7, typical of composites sintered from compacts with $d_T \geq 75\%$ oxygen is also a constituent of phase 2.

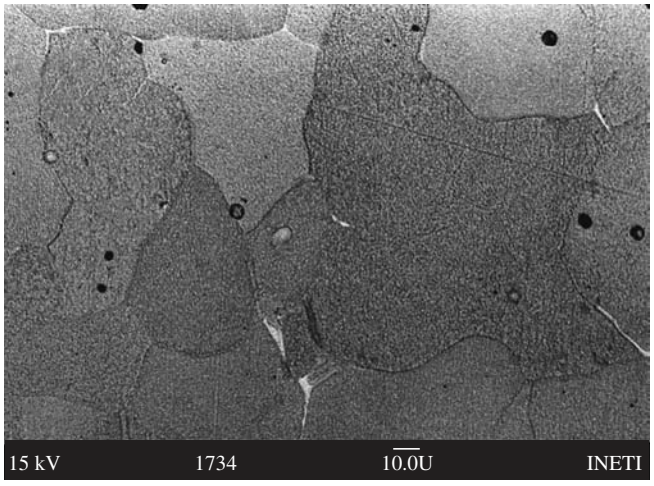

(a)

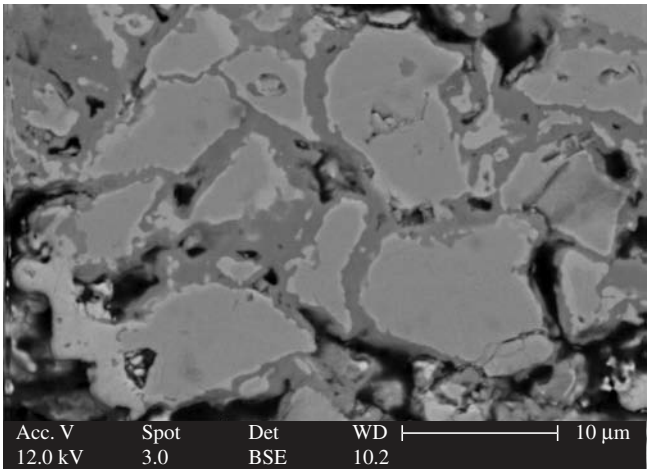

(b)

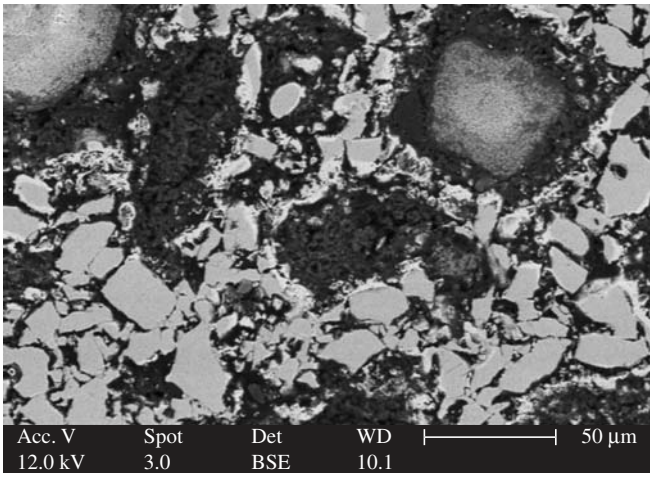

(c)

Figure 4. Densification achieved in materials sintered from: a) TiH_2 monolithic (82%d_T); and b,c) TiH_2/50v%HAP (86%d_T) composite.

HAP partial decomposition into CaO and $Ca_4O(PO_4)_2$ (TTCP) and some Ti as Ti_2O and also still as titanium hidride ($TiH_{0.71}$) are visible in Figure 7. The constituents interactions resulted in the formation of $CaTiO_3$ and Ti_4P_3 and a set of peaks compatible with the PDF 45-0888 published for Ti_5P_3[12]. However no set of peaks was identified to correlate to the diffraction file of the compound $CaTi_4(PO_4)_2$ (PDF 49-0787), which is the only one containing Ti, Ca and P with a published file. The composites sintered from compacts with $d_T < 75\%$ presented the same phases with the exception of Ti_5P_3, and $CaTiO_3$ was detected in only one sample.

The XRD analysis of the material illustrated in Figure 4a), sintered from monolithic TiH_2 (82%d_T), revealed only Ti_α.

The mean geometrical and true densities of the sintered composites for the two groups of green compacts density (above or below 75%d_T) are given in Table 1. It should be noted that the amount of powder available for each true density measurement was much lower than the recommended for the type of equipment used and consequently, the calculated porosities must only be taken as "estimates".

In a previous work[11] similar composites processed from commercially pure titanium powder (CTA) with d_{50} = 110 µm were produced. The mixtures compacted to about 60%d_T and vacuum sintered at 1150 °C resulted in sintered composites with microstructures different from those presented in this work, since all HAP appeared in agglomerates of dimensions near to those of the Ti grains and with cracks, as can be seen in Figure 8. Therefore no areas equivalent to those seen in Figure 4b) were found. Another microstructural difference was related to the appearance of the phase with Ti and P, generally thicker and more porous, as shown in Figure 8b). The true density of these sintered composites was not measured due to the insufficient amount available.

XRD spectra of these composites (Figure 9) are similar to the ones of composites processed from TiH_2 with the same compaction density. The compounds detected were: HAP, decomposition products CaO and TTCP, and only Ti_4P_3 resultant from the interaction between the constituents; Ti appears as Ti_α and as Ti_2O.

4. Discussion

The use of TiH_2 showed some advantage as compared to the previous use of Ti powders: the closer median sizes of TiH_2 and HAP allowed an easier obtention of homogeneous mixtures and the tendency for the HAP to form large agglomerates was decreased due to the presence of the TiH_2 fines (around 10 wt. (%) < 3 µm); also the TiH_2/HAP mixtures were slightly more compressible than the Ti/HAP ones.

Although a high degree of densification was expected for the TiH_2 based composites, it was found that the increased sinterability of TiH_2 as compared with Ti[14] was affected by the presence of HAP. The purpose of the present work being the evaluation of the Ti-HAP interactions as extensively as possible, full densification of the com-

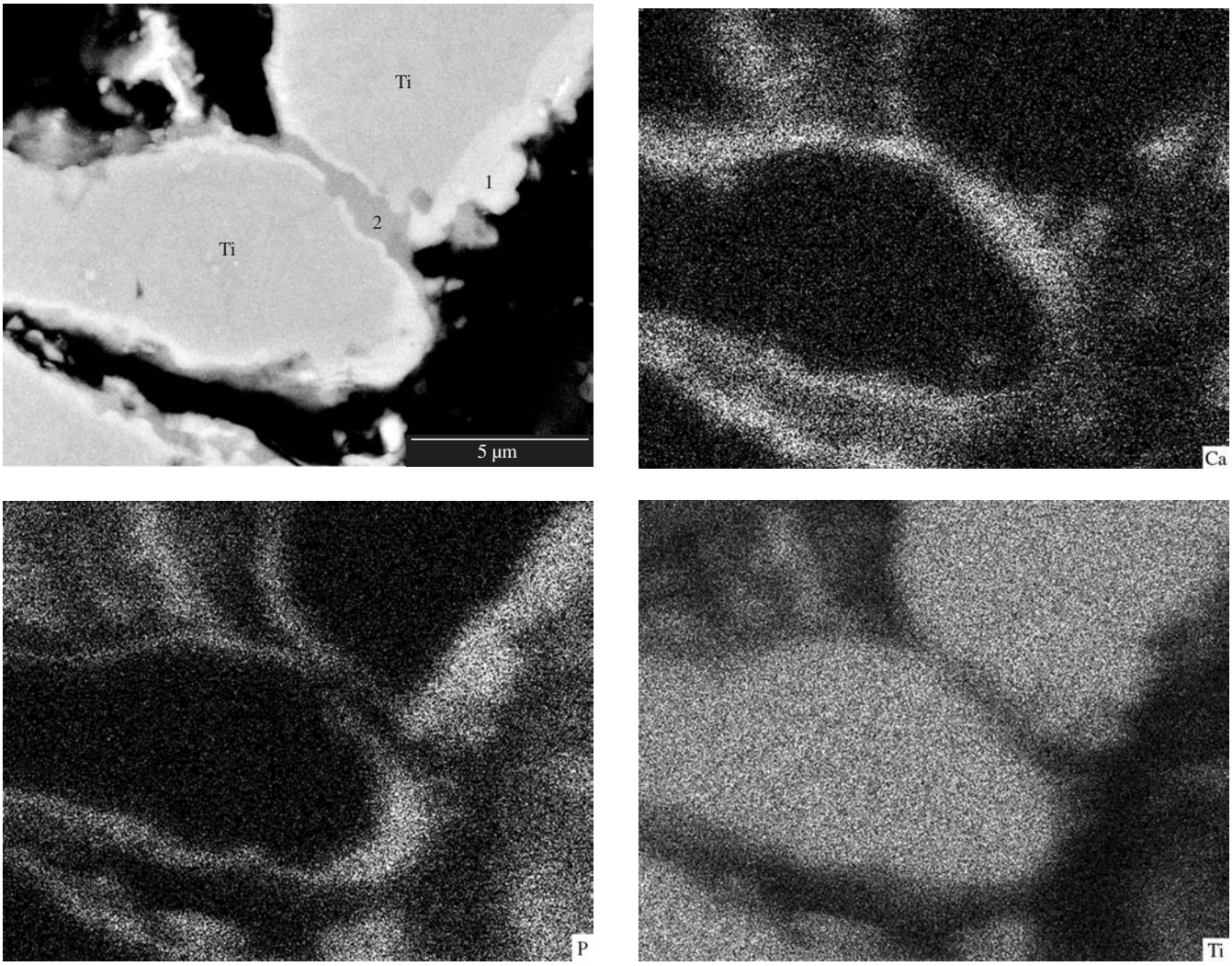

Figure 5. Backscattered electron image (SEM) and correlated XR maps (EDS) from the Ti/HAP composite sintered from TiH_2/HAP compacted with 77%d_t. 1: Ti-P; 2: Ti-Ca.

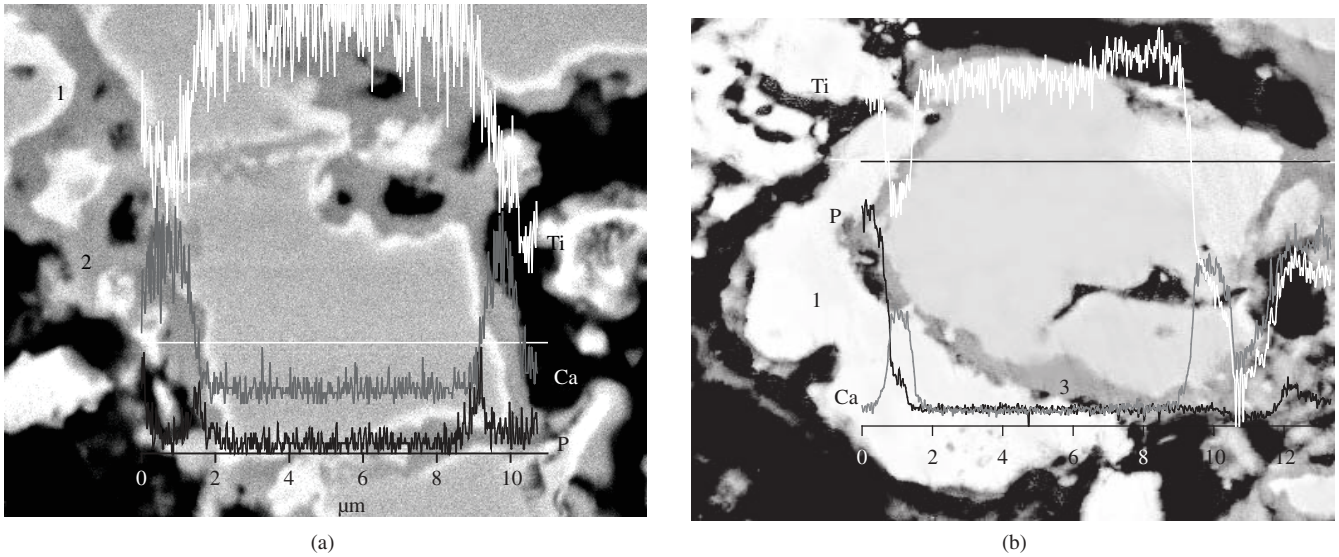

(a) (b)

Figure 6. Ti, Ca and P XR profiles (EDS) from composites sintered from TiH_2/HAP greens with: a) 77% d_t; and b) 82% d_t. 1: Ti-P; 2: Ti-Ca; 3: Ti-Ca-P.

posites was desirable for a better understanding of the microstructural features as well as to achieve acceptable mechanical properties.

The amount of porosity remaining in both types of sintered composites could not be compared, because it was not measured for the Ti/50v%HAP ones and also due to the uncertainty of the values calculated in the present work. Quantification of the total porosity through standard image analysis procedures was considered but not found meaningfull due to the lack of an extensive previous effort to improve the samples metallographic preparation. However visual estimates seem to indicate that, for similar greens $\%d_T$, the final porosity is indeed less for the TiH_2 based composites than for the Ti based ones.

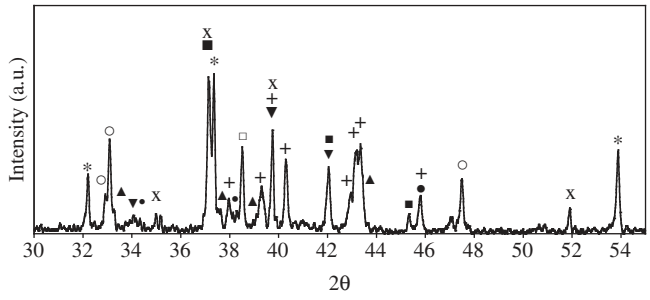

Figure 7. Typical XRD spectrum of composites sintered from TiH_2/HAP compacted with $d_T \geq 75\%$. Phases (PDF Nº.): ▼ HAP (9-0432); ■ $TiH_{0.71}$ (40-0980); * CaO (37-1497); + TTCP (25-1137); ● Ti_4P_3 (22-0944); ▲ Ti_5P_3 (45-0888); ○ $CaTiO_3$ (22-0153); x Ti_2O (11-0218), □ Ti_α (44-1294).

Table 2 summarizes the phases detected in the vacuum sintered composites mixtures as well as in the materials sintered from the monolithic constituents TiH_2 and HAP. All composites show: 1) strong decomposition of the HAP (not found in the monolithic) with the consequent formation of CaO and TTCP; 2) the presence of Ti_2O[15] which suggests that even with the dynamic vacuum of around 10^{-3} Pa the oxidizing effect brought by the HAP decomposition was present; and 3) formation of Ti_4P_3. Additionally, in the TiH_2 based composites incomplete H_2 release was found since $TiH_{0.71}$ was also detected besides the Ti_α, as well as formation of $CaTiO_3$ and Ti_5P_3 in the composites with green density $\geq 75\%d_T$. The amount of final Ti_α detected in the Ti based composites (Figure 9) seems to be much less than that in the TiH_2 based ones (Figure 7) which suggests a higher "consumption" of Ti in the former. However this did not result in a larger amount or variety of Ti containing reaction products since only Ti_4P_3 was detected in the Ti based composites while, for a similar degree of green compaction ($60\%d_T$), the TiH_2 based composites already showed some $CaTiO_3$, as mentioned before.

The intense HAP decomposition found in the present work is consistent with other authors findings of Ti promoting HAP decom-

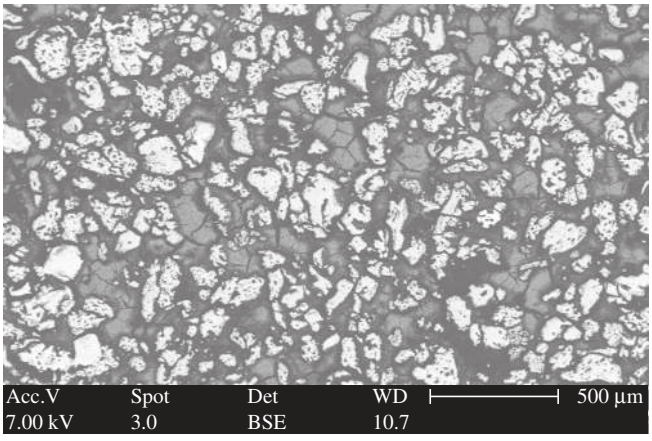

(a)

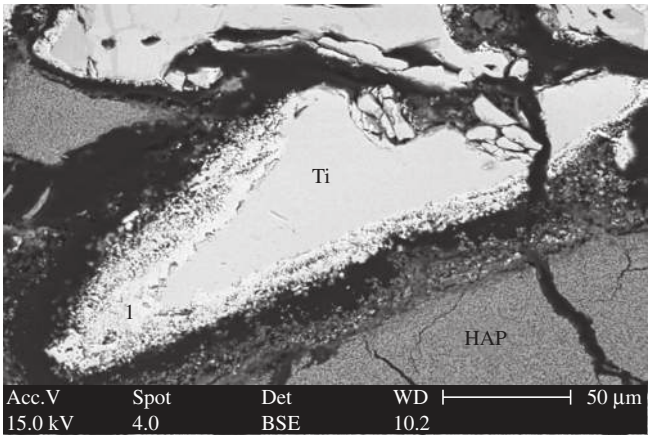

(b)

Figure 8. Microstructural characteristics (SEM) of Ti/50v%HAP composites sintered from greens with 60% d_T. 1: Ti-P.

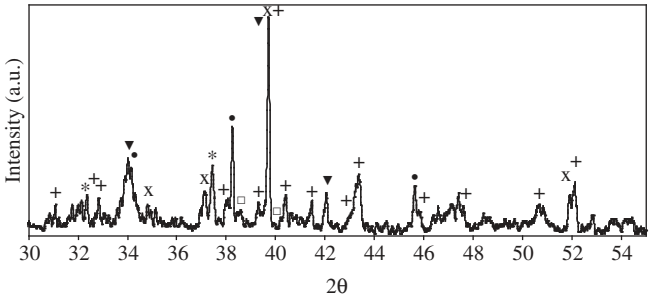

Figure 9. Typical XRD spectrum of Ti/50v%HAP sintered from greens with $60\%d_T$. Phases (PDF Nº.): ▼ HAP (9-0432); * CaO (37-1497); + TTCP (25-1137); ● Ti_4P_3 (22-0944); x Ti_2O (11-0218), □ Ti_α (44-1294).

Table 1. Geometrical and true densities of the composites sintered from TiH_2/50v%HAP.

Green density ($\%d_T$)	Mean sintered density ($g.cm^{-3}$)		Porosity (calculated, %)
	Geometrical (P/V)	He pycnometer	
< 75%	2.2	3.2	31
≥ 75%	3.0	3.9	23

Table 2. Phases detected (XRD) on compacts vacuum sintered at 1150 °C.

Starting material		Phases detected
TiH_2		Ti_α
HAP[11]		HAP, α - TCP (minor)
TiH_2/50v%HAP	$< 75\%d_T$	Ti_α, Ti_2O, $TiH_{0.71}$, HAP, CaO, TTCP, Ti_4P_3
	$\geq 75\%d_T$	Ti_α, Ti_2O, $TiH_{0.71}$, HAP, CaO, TTCP, Ti_4P_3, Ti_5P_3, $CaTiO_3$
Ti/50v%HAP[11]	$60\%d_T$	Ti_α, Ti_2O, HAP, CaO, TTCP, Ti_4P_3

position at temperatures lower than the decomposition temperatures of the corresponding monolithic powders, starting even as low as at 800 °C[7,10].

The resulting CaO suggests that the used HAP, supplied as stoichiometric, has evolved to a Ca/P ratio higher than 1.67 due to the Ti_4P_3 and Ti_5P_3 formation. According to recent studies carried out on hydroxyapatites with different Ca/P ratios[8,13], when HAP decomposition takes place the formation of CaO occurs if there is an excess of Ca while, for stoichiometric or Ca defficient HAP, α - and/or β - TCP (TCP-$Ca_3(PO_4)_2$) as well as TTCP will result instead. CaO formation is to be avoided in implant materials since it decreases the mechanical resistance and can cause material decohesion due to transformation into $Ca(OH)_2$, besides affecting the rate and extension of HAP dissolution which typically is of the order of 15 to 30 μm per year[3].

The formed Ti phosphides result from the diffusion of P ions into the Ti particles, this being favoured by a reducing or non-oxidizing sintering atmosphere[16]. A Ti_3P_2 phase was detected at the interface of a HAP coated Ti alloy[17] and stated to have contributed to the good coating/substrate adhesion determined, together with the Ca titanates also formed; in this particular example the coating process involved the use of temperatures above the HAP melting point. Ti_xP_y type phases as well as $CaTiO_3$ were also detected in Ti/HAP PM composites hot pressed at 20 MPa between 1000 and 1200 °C in argon atmosphere[9] and apparently did not suffer degradation during the subsequent 14 days tests *in vitro*. It seems therefore reasonable to expect that the Ti phosphides and Ca titanates formed in the present work can also be considered to contribute to improve the Ti/HAP bonding and without introducing deleterious effects in physiological tests.

According to literature the Ca titanates $CaTiO_3$ and $CaTi_2O_5$ are formed through reactions between HAP and TiO_2 in vacuum, both when the TiO_2 was intentionally added[7] or when it resulted from the oxidation of metallic Ti in Ti/HAP composites[10] according to the reaction:

$$Ti + 2H_2O \rightarrow TiO_2 + 2H_2 \quad (1)$$

where the H_2O is suggested to result from the loss of part of the OH^- of the HAP which occurs from 800 °C onwards. The reaction between HAP and TiO_2 yields Ca titanates, TCP and H_2O[7,10] according to Equations 2 or 3:

$$Ca_{10}(PO_4)_6(OH)_2 + TiO_2 \rightarrow 3Ca_3(PO_4)_2 + CaTiO_3 + H_2O \quad (2)$$

$$Ca_{10}(PO_4)_6(OH)_2 + 2TiO_2 \rightarrow 3Ca_3(PO_4)_2 + CaTi_2O_5 + H_2O \quad (3)$$

In the present work TCP was not detected probably due to subsequent decomposition into TTCP. It is to be noted that the CaO-TiO_2 phase diagram[18] shows that $CaTiO_3$ formation can also occur through the combination of these two oxides.

The oxidation of Ti in a different proportion than the one shown in Equation 1 can explain both the incomplete dehydrogenation of the TiH_2 and the detection of Ti_2O in all composites; oxidation was probably stronger in the Ti based composites although it can not be seen by comparing Figures 7 and 9 spectra.

It seems then possible to conclude that the formation of Ca titanates and Ti phosphides is relevant for the composites densification since they contribute to the metal/ceramic bonding, being nevertheless necessary to carry out an exhaustive study of the biocompatibility and bioactivity of these materials. The sintering conditions need to be modified in order to decrease the extension of HAP decomposition and formation of other compounds. The use of Ca deficient HAP and/or a non-conventional type of sinterization with short times at temperature (e.g. microwave sintering) could be adequate processing alternatives for Ti-HAP PM composites. On the other hand, for functionally graded materials and identical sintering conditions, HAP decomposition will previsibly be more limited.

5. Conclusions

When producing Ti/50v%HAP composites (from either TiH_2 or Ti powders) by sintering in vacuum at 1150 °C, the use of these conditions which are favourable for Ti densification resulted in HAP decomposition into CaO and TTCP and formation of several Ti-HAP interaction products. Ti_4P_3 was formed in all composites. Ti_5P_3 and $CaTiO_3$ were formed in TiH_2/HAP composites with green density ≥ 75%d_T thus showing the influence of the initial compaction in the constituents interaction. For similar green densities of around 60%d_T, the detection of $CaTiO_3$ only in TiH_2 based composites suggests a higher degree of Ti-HAP interaction in these composites than in the Ti based ones. The use of TiH_2 instead of Ti powders showed some advantage in terms of an easier manipulation of their mixtures with HAP, obtention of finer microstructures and conservation of the Ti_α phase.

The use of a Ca deficient HAP in order to avoid CaO formation, associated to another type of sintering which minimizes HAP decomposition are suggested alternatives for the fabrication of these type of composites.

Acknowledgments

The authors are gratefull to CTA/IAE (Materials Division) and CBPF for providing the TiH_2 and HAP powders, respectively.

References

1. Long M, Rack HJ. Review Titanium alloys in total joint replacement – a materials science perspective. *Biomaterials*. 1998; 19(18):1621-1639.
2. Yang CY, Wang BC, Chang E, Wu JD. The influences of plasma spraying parameters on the characteristics of hydroxyapatite coatings: a quantitative study. *Journal of Materials Science: Materials in Medicine*. 1995; 6(5):249-257.
3. Suchanek W, Yoshimura M. Processing and properties of hydroxyapatite-based biomaterials for use as hard tissue replacement implants. *Journal of Materials Research*. 1998; 13(1):94-117.
4. Zheng X, Huang M, Ding C. Bond strength of plasma-sprayed hydroxyapatite/Ti composite coatings. *Biomaterials*. 2000; 21(8):841-849.
5. Chenglin C, Jingchuan Z, Zhongda Y, Shidong W. Hydroxyapatite-Ti functionally graded biomaterial fabricated by powder metallurgy. *Materials Science and Engineering* A. 1999; 271(1-2):95-100.
6. Watari F, Yokoyama A, Omori M, Hirai T, Kondo H, Uo M et al. Biocompatibility of materials and development to functionally graded implant for bio-medical application. *Composites Science and Technology*. 2004; 64(6):893-908.
7. Weng J, Liu X, Zhang X, Ji X. Thermal decomposition of hydroxyapatite structure induced by titanium and its dioxide. *Journal of Materials Science Letters*. 1994; 13(3):159-161.
8. Chu C, Lin P, Dong Y, Xue X, Zhu J, Yin Z. Fabrication and characterization of hydroxyapatite reinforced with 20 vol% Ti particles for use as hard tissue replacement. *Journal of Materials Science: Materials in Medicine*. 2002; 13(10):985-992.
9. Ning CQ, Zhou Y. In vitro bioactivity of a biocomposite fabricated from HA and Ti powders by powder metallurgy method. *Biomaterials*. 2002; 23(14):2909-2915.
10. Yang Y, Kim KH, Agrawal CM, Ong JL. Interaction of hydroxyapatite-titanium at elevated temperature in vacuum environment. *Biomaterials*. 2004; 25(15):2927-2932.
11. Silva A, Carvalho MH. Atmosphere and constituint reaction effects on titanium-hydroxyapatite sintered composites (poster P3.21). In: Martins R, Dias C, Fortunato E, Ferreira I, Godinho H, Monteiro R, editors. *Materiais 2003 – a materials science forum*. Book of Abstracts of the XI Meeting of the Portuguese Materials Society; 2003 April 14-16; Caparica, Portugal. Caparica: Departamento de Ciência dos Materiais, Faculdade de Ciências e Tecnologia, Universidade Nova de Lisboa; 2003. p. 175.

12. International Center for Diffraction Data. *Powder Diffraction File-2*. ISSN 1084-3116. [CD-ROM]. Pennsylvania: ICDD; 2003.
13. Raynaud S, Champion E, Bernache-Assollant D, Thomas P. Calcium phosphate apatites with variable Ca/P atomic ratio I. Synthesis, characterisation and thermal stability of powders. *Biomaterials*. 2002; 23(4):1065-1072.
14. Senkov ON, Froes FH. Thermohydrogen processing of titanium alloys. *International Journal of Hydrogen Energy*. 1999; 24(6):565-576.
15. Massalski TB, editor-in-chief. *Binary Alloy Phase Diagrams*. v. 2. Metals Park, Ohio: American Society for Metals; 1986.
16. Ji H, Ponton CB, Marquis PM. Microstructural characterization of hydroxyapatite coating on titanium. *Journal of Materials Science: Materials in Medicine*. 1992; 3(4):283-287.
17. Lusquiños F, Pou J, Arias JL, Boutinguiza M, León B, Amor MP et al. The role of processing parameters on calcium phosphate coatings obtained by laser cladding. In: Barbosa MA, Monteiro FJ, Correia R, Leon B, editors. *Bioceramics 16. Proceedings of the 16th International Symposium on Ceramics in Medicine; 2003 Nov 6-9; Porto, Portugal. Key Engineering Materials 254-256*; Switzerland: Trans Tech Publications; 2004. p. 371-374.
18. Levin EM, Robbins CR, McMurdie HF. *Phase diagrams for ceramists*. 2nd edition. Columbus, Ohio: The American Ceramic Society; 1969. p. 104.